Salih *et al. Int J Concr Struct Mater* (2025) 19:132
https://doi.org/10.1186/s40069-025-00876-z

International Journal of Concrete Structures and Materials

RESEARCH

Open Access

Post-fire Mechanical Behaviour of Concrete Reinforced with Phragmites Australis Fibres

Baydaa Hamdi Salih[1], Sadoon Abdallah[1*], Mohammed T. Nawar[1], Ali J. Ali[2], Mizi Fan[2] and Ameer A. Hilal[1]

Abstract

The use of natural fibres as concrete reinforcement has gained increasing attention due to their environmental benefits, renewability, and cost-effectiveness. This study investigates the post-fire mechanical behaviour of concrete reinforced with Phragmites australis fibres (PAF), a locally available and sustainable material. Concrete mixes containing 0%, 0.5%, 1%, 1.5%, and 2% fibre volume fractions were exposed to temperatures up to 600 °C for 2 h to simulate fire conditions. The effects of fibre content and temperature were assessed through measurements of slump, compressive strength, splitting tensile strength, flexural strength, and ultrasonic pulse velocity (UPV). Results showed that PAF-reinforced concrete retained considerable strength and integrity up to 400 °C, with a pronounced reduction observed at 600 °C due to fibre degradation and microcrack propagation. Regression models developed from the experimental data demonstrated strong correlations between fibre dosage, temperature, and residual mechanical properties. The analysis identified an optimal fibre content between 0.5% and 1%, which provided the best balance between thermal stability and mechanical performance. These findings highlight the potential of Phragmites australis fibres as an effective and sustainable reinforcement for improving the fire resistance of concrete structures.

Keywords Phragmites australis, Post-fire, Sustainable construction materials, Mechanical properties, High temperatures

1 Introduction

Concrete structures are often exposed to elevated temperatures during fire incidents, which can significantly compromise their mechanical and durability properties (Altunişik et al., 2023; Amer et al., 2023; Chun et al., 2022). Under such conditions, concrete undergoes a series of physicochemical changes, including moisture evaporation, thermal incompatibility between aggregates and cement paste, and the formation of microcracks all of which result in reduced strength and stiffness (Zalhaf et al., 2024; Zalhaf, 2025). These transformations pose serious concerns for structural safety, especially in critical infrastructure and high-performance buildings (Eng & Kim, 2025; Lee et al., 2025). One widely adopted approach to mitigate thermal degradation and improve the fire resistance of concrete is the incorporation of fibres (Han et al., 2024; Zhao et al., 2025). Fibres can help delay crack formation, control crack propagation, and reduce the risk of explosive spalling by improving pore connectivity and dissipating thermal stresses (Abdallah et al., 2017; Alsaif & Abbas, 2025; Liang et al., 2025).

Various synthetic and metallic fibres have demonstrated such benefits under elevated temperatures. For instance, Hung et al. (2024) reported that UHPC reinforced with hybrid steel and polypropylene fibres maintained tensile strain-hardening behaviour up to 700 °C and showed increased strength up to 300 °C despite microstructural degradation at higher temperatures. Polypropylene fibres effectively mitigated spalling above

Journal information: ISSN 1976-0485 / eISSN 2234-1315

*Correspondence:
Sadoon Abdallah
sadoon.m.abdullah@uoanbar.edu.iq
[1] Civil Engineering Department, College of Engineering, University of Anbar, Ramadi, Iraq
[2] College of Engineering, Design and Physical Sciences, Brunel University London, Uxbridge, Middlesex UB8 3PH, UK

300 °C by creating microchannels for pressure release, although they slightly increased porosity and water absorption. Noumowe (2005) also found that adding 1.8% polypropylene fibres improved both compressive and tensile strengths of concrete at 200 °C. Similarly, Gencel et al. (2022) observed strength gains in concrete with 3% basalt fibres after exposure to 800 °C. Amin et al. (2020) reported up to a 76% improvement in compressive strength of lightweight concrete when reinforced with glass and polypropylene fibres at 400 °C. Furthermore, Talaei and Mostofnejad (2021) noted that steel fibres could enhance residual compressive strength by 20–30% at 400 °C and 800 °C, respectively. In parallel, increasing attention has been directed toward the use of natural (bio-based) fibres in concrete due to their low environmental impact, renewability, and affordability. Fibres such as coir, sisal, jute, hemp, and flax have been shown to enhance tensile and flexural properties and reduce thermal-induced spalling. Aluko et al. (2020) demonstrated that lignocellulosic natural fibres contributed to improved thermal performance and reduced spalling in ultra-high-performance concrete (UHPC). Zhang et al. (2020), exploring jute fibre as an alternative to polypropylene in thermally exposed UHPC, observed improved compressive strength at 200 °C, but a significant decline at temperatures exceeding 400 °C. Their findings also highlighted the fibre shrinkage under heat, which altered the microstructure and permeability of the composite. Ozawa et al. (2016) reported that while jute-reinforced high-strength concrete (HSC) initially showed strength reductions at 100 °C, it recovered full strength by 200–300 °C, and prevented explosive spalling.

However, natural fibres' performance under heat is highly variable due to their heterogeneous structure and sensitivity to degradation (Elfaleh et al., 2023; Thomason & Rudeiros-Fernández, 2021). Unlike steel or synthetic fibres, the mechanical stability of bio-fibres under thermal stress cannot be predicted reliably. Their behaviour is affected by several parameters, including fibre type, dosage, treatment method, matrix composition, aggregate type, and environmental exposure conditions, such as heating rate and cooling regime (Aluko et al., 2020). Moreover, fibre–matrix bonding plays a crucial role in determining the effectiveness of fibre reinforcement at elevated temperatures. Alkali treatment (e.g., using NaOH) is a commonly used method to enhance fibre–matrix interaction by removing amorphous materials, such as hemicellulose and lignin, increasing surface roughness, and improving thermal stability (Dash et al., 2023; Elfaleh et al., 2023; Ye et al., 2018).

Despite growing interest in natural fibre-reinforced concrete (NFRC), there remains limited information on the thermal properties and high-temperature performance of Phragmites australis (common reed) fibres in cementitious composites. Phragmites australis (PA) is an abundant and fast-growing plant found along riverbanks and wetlands worldwide (Khatib, Jamal et al., 2023; Khatib, Jamal M. et al., 2023). In contrast to traditional natural fibres such as jute, coir, or sisal, Phragmites australis (PA) fibres have a unique hollow structure and a comparatively elevated silica content, potentially improving their thermal stability and crack-bridging ability (Khatib, Jamal et al., 2024). These characteristics enhance post-cracking energy absorption and may mitigate the danger of explosive spalling at increased temperatures. Furthermore, PA fibres have a favourable response to alkali treatment (e.g., NaOH), enhancing fibre–matrix adhesion by augmenting surface roughness and eliminating amorphous constituents. This improved interfacial contact enhances mechanical performance, especially in tensile and flexural applications (Abdallah et al., 2025). Its widespread availability and biodegradability make it an appealing candidate for sustainable construction materials (Khatib, Jamal et al., 2024; Shon et al., 2019).

While a few studies (Durant et al., 2020; Khatib, Jamal M. et al., 2023a, 2023b; Khatib, Jamal et al., 2024; Shon et al., 2019) have explored the mechanical benefits of PA fibres under ambient conditions, little is known about their performance when exposed to elevated temperatures. This knowledge gap is particularly important given the unpredictable degradation behaviour of bio-fibres under heat (Aluko et al., 2020). Understanding the residual mechanical properties of PAF-reinforced concrete after thermal exposure is essential for developing effective, eco-friendly alternatives to traditional fire-resistant materials.

This study investigates the post-heating mechanical behaviour of concrete reinforced with alkali-treated Phragmites australis fibres. The properties evaluated include slump, compressive strength, splitting tensile strength, flexural strength, and ultrasonic pulse velocity (UPV), both before and after exposure to temperatures up to 600 °C. The results offer insights into the feasibility of using PA fibres to enhance the fire resilience of concrete while promoting sustainable material use.

2 Experimental Program

2.1 Materials

2.1.1 Cement

Ordinary Portland Cement (OPC), classified as CEM I 42.5R, was used as the primary binder. It had a specific gravity of approximately 3.15 and a Blaine fineness of 386 m^2/kg. This type of cement is suitable for structural applications due to its high early strength and compatibility with various aggregates and additives.

2.1.2 Fine and Coarse Aggregates

Clean, natural river sand with a fineness modulus of 2.6 and a specific gravity of 2.63 was employed as the fine aggregate. The sand was thoroughly washed to remove silt, clay, and organic impurities and met the grading requirements of ASTM C33 (Standard, 2018). The coarse aggregate consisted of crushed gravel with a nominal maximum size of 12.5 mm, specific gravity of 2.70, and an aggregate crushing value below 30%, indicating good mechanical performance. It was also in compliance with ASTM C33 standards.

2.1.3 Phragmites Australis Fibres (PAF)

Fibres were extracted from mature Phragmites australis plants collected along the Euphrates River. Figure 1 illustrates the sequential stages of fibre preparation, including harvesting, cutting, treatment, and drying. After air-drying, the stems were chopped using a mechanical cutter into segments of 40–50 mm in length, determined through preliminary tests as optimal for concrete reinforcement. This length balances fibre dispersion with effective crack-bridging capability.

2.2 Fibre Treatment

To improve fibre–matrix adhesion, an alkaline treatment was conducted. The PAF were immersed in a 1% sodium hydroxide (NaOH) solution for 24 h at room temperature. This process removed hemicellulose, waxes, and surface impurities and enhanced surface roughness. Fibres were then thoroughly rinsed with clean water until a neutral pH was achieved and oven-dried at 60 °C for 24 h, as shown in Fig. 1.

2.3 Mix Proportions

A control concrete mix targeting a 28-day compressive strength of 40 MPa was designed with a constant water-to-cement (w/c) ratio of 0.50. Table 1 presents the mix proportions. PAF were added in varying amounts: 0% (control), 0.5%, 1.0%, 1.5%, and 2.0% by volume fraction. No chemical admixtures were used, ensuring that the fibres' influence on workability and mechanical performance could be clearly assessed. The selection of fibre contents was based on prior studies by (Khatib, Jamal et al., 2024; Ramadan et al., 2023)

Table 1 Concrete mix proportions of all mixes

Mix ID	Fibre Content (kg/m^3)	Cement	Fine aggregate	Coarse aggregate	Water
PA0	0.00	375	795	970	185
PA0.5	3.33	375	795	970	185
PA1.0	6.65	375	795	970	185
PA1.5	9.98	375	795	970	185
PA2.0	13.28	375	795	970	185

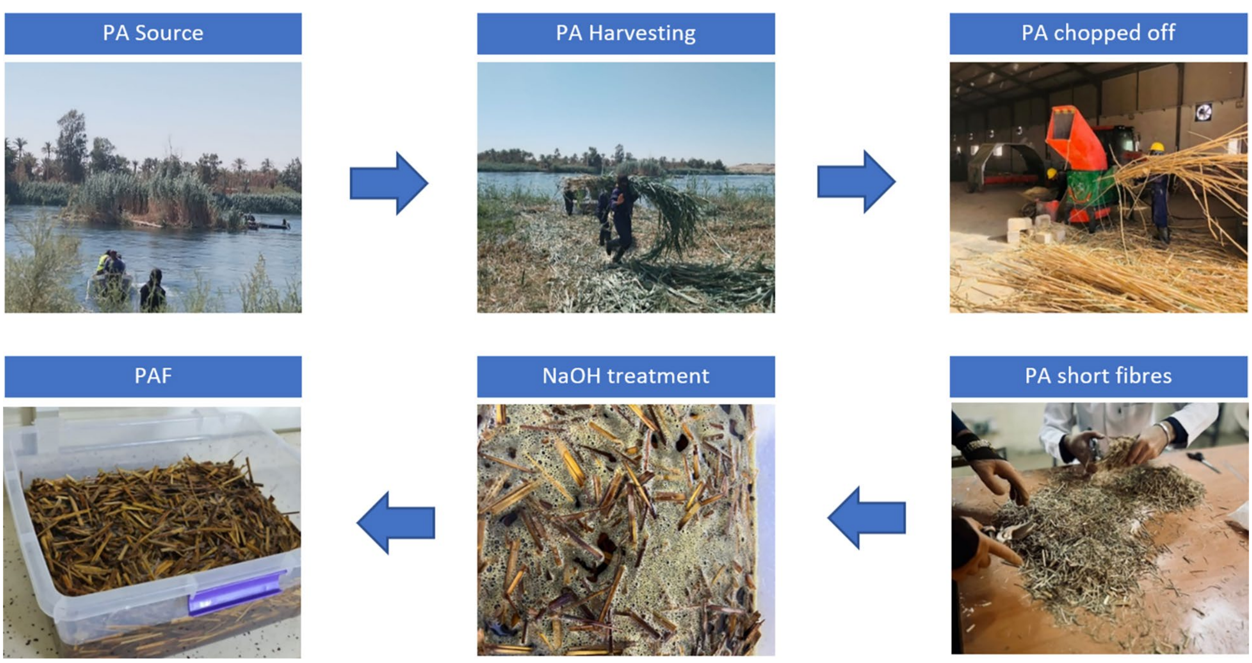

Fig. 1 Process of preparing Phragmites australis fibres (PAF) for concrete reinforcement: from natural harvesting along riverbanks, drying and chopping, to alkaline treatment with NaOH, rinsing, and final drying before incorporation into the concrete mix

indicating that contents above 2% can lead to severe reductions in workability and mechanical integrity due to fibre clustering and air entrapment. All raw materials were batched by weight and converted to volume using respective specific gravities. The fresh concrete densities ranged from 2100 to 2400 kg/m^3.

2.4 Mixing Procedure

Mixing was carried out using a 60-L tilting pan mixer. Dry materials (cement, sand, and gravel) were first mixed for 1 min. Then, 75% of the total mixing water was gradually added over 1 min, followed by 2 min of continuous mixing. The pre-measured fibres were slowly introduced, followed by the remaining 25% of water, and mixed for an additional 2 min to ensure even distribution. Mixes with higher fibre contents (1.5% and 2%) exhibited noticeably reduced workability but remained sufficiently cohesive for placement with mechanical vibration.

2.5 Specimen Preparation and Curing

The specimens were produced in compliance with the ASTM and BS standards. Compressive strength was assessed using 100 mm cube specimens in accordance with BS EN 12390-3:2009 (EN, 2009), evaluated at curing ages of 7, 14, and 28 days. Flexural strength was conducted on 100 × 100 × 500 mm prisms using four-point bending in line with (BS EN 12390-5, 2009), while splitting tensile strength was determined on 150 × 300 mm cylindrical specimens following ASTM C496-11 (American Society for Testing and Materials. Committee C-9 on Concrete and Concrete Aggregates, 2011). Moulds were filled in stages and compressed on a vibrating table for around 15–20 s each layer to achieve homogeneous consolidation. After casting, specimens were covered with plastic sheets for 24 h, demoulded, and then cured in water at 23 ± 2 °C until testing. In summary, all mechanical tests employed standard specimen sizes 100 mm cubes for compressive strength, 150 × 300 mm cylinders for splitting tensile strength, and 100 × 100 × 500 mm prisms for flexural strength with dimensional tolerances maintained within ± 2 mm in accordance with the respective standards. Each reported value represents the mean of three identical specimens.

2.6 Heating Scheme

To assess the post-heating mechanical behaviour of the concrete mixes, a controlled heating regime was applied to selected specimens. After 28 days of standard water curing, the specimens were dried at ambient conditions for 24 h to minimize thermal shock. They were then placed in a programmable muffle furnace, as shown in Fig. 2. The temperature was increased at a steady rate of 5 °C per minute until target temperatures of 200 °C, 400 °C, and 600 °C were reached (Fig. 3). Each target temperature was held constant for 2 h to ensure uniform thermal exposure. A set of specimens was retained at ambient laboratory temperature to serve as a reference group for comparison. After heating, all specimens were allowed to cool gradually in the furnace to avoid rapid thermal contraction, then tested for mechanical properties within 24 h. This heating scheme was designed to simulate realistic fire exposure scenarios and assess the thermal stability of concrete reinforced with Phragmites australis fibres.

Fig. 2 Electric furnace used for thermal exposure of concrete specimens

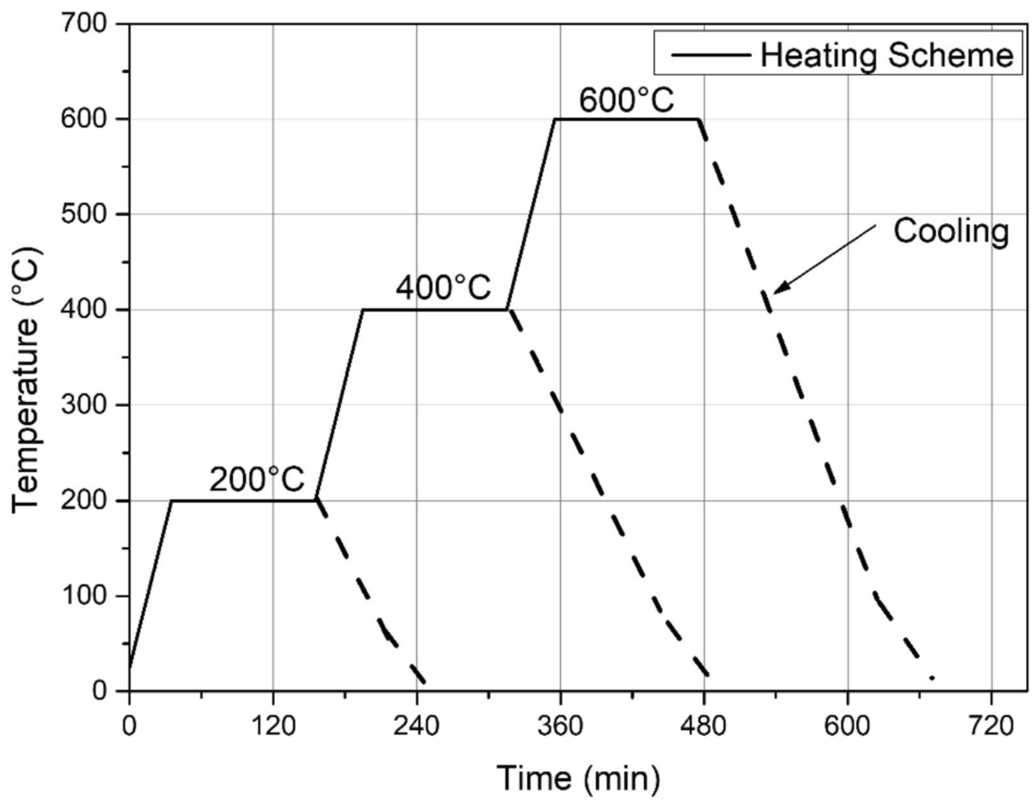

Fig. 3 Temperature–time curves recorded during the furnace heating process

3 Results and Discussion

3.1 Fresh Properties

The slump test results of the control mix (PA0%) and concrete mixes containing Phragmites australis fibres (PAF) are presented in Fig. 4. The findings of the slump test showed a definite negative correlation between the workability of concrete and the amount of Phragmites australis fibre (PAF). With the maximum slump value of 7.5 cm, the fibre-free control mix (CM) demonstrated exceptional workability. The droop somewhat diminished to 7.3 cm upon the addition of PAF at 0.5%, indicating a negligible effect on fresh characteristics. The slump values gradually decreased to 6.8 cm, 6.4 cm, and 5.7 cm, respectively, as the fibre content rose to 1%, 1.5%, and 2%.

A number of issues related to the incorporation of natural fibres can be justified for this decrease in workability. First, the mix's capacity to compress and settle under its own weight is restricted by the fibrous network's increased internal friction and flow resistance. Furthermore, PAF's high water absorption capacity and surface roughness, may further diminish free water in the mixture, giving it a stiffer consistency. These results are in line with patterns shown in earlier research on various natural fibres, including flax, jute, hemp, and coir (e.g.,Abdalla et al., 2023; Chen et al., 2023; Islam & Ahmed, 2018; Mohammed et al., 2024), where a higher fibre content resulted in less slump and increased compaction sensitivity.

All mixes retained enough workability for casting, especially with mechanical vibration, even if slump decreased. This suggests that PAF may be added to concrete at reasonable doses (≤ 1.5%) without the need for chemical admixtures. Workability, however, can become a limiting issue at higher fibre percentages (2%), necessitating changes to the mix design or the addition of plasticisers.

3.2 Hardened Properties

3.2.1 Mass Loss

The mass loss results of concrete specimens reinforced with varying contents of Phragmites australis fibres (PAF) exposed to elevated temperatures (200–600 °C) indicate a clear temperature-dependent trend (see Fig. 5). At 200 °C, all mixes exhibited relatively low mass loss, with PA0.5% showing the highest (3.51%) and PA1% the lowest (1.34%), suggesting some moisture evaporation and initial organic degradation. Similar trend was observed by (Mihoub et al., 2020).

At 400 °C, mass loss increased significantly across all mixes due to decomposition of hydration products and

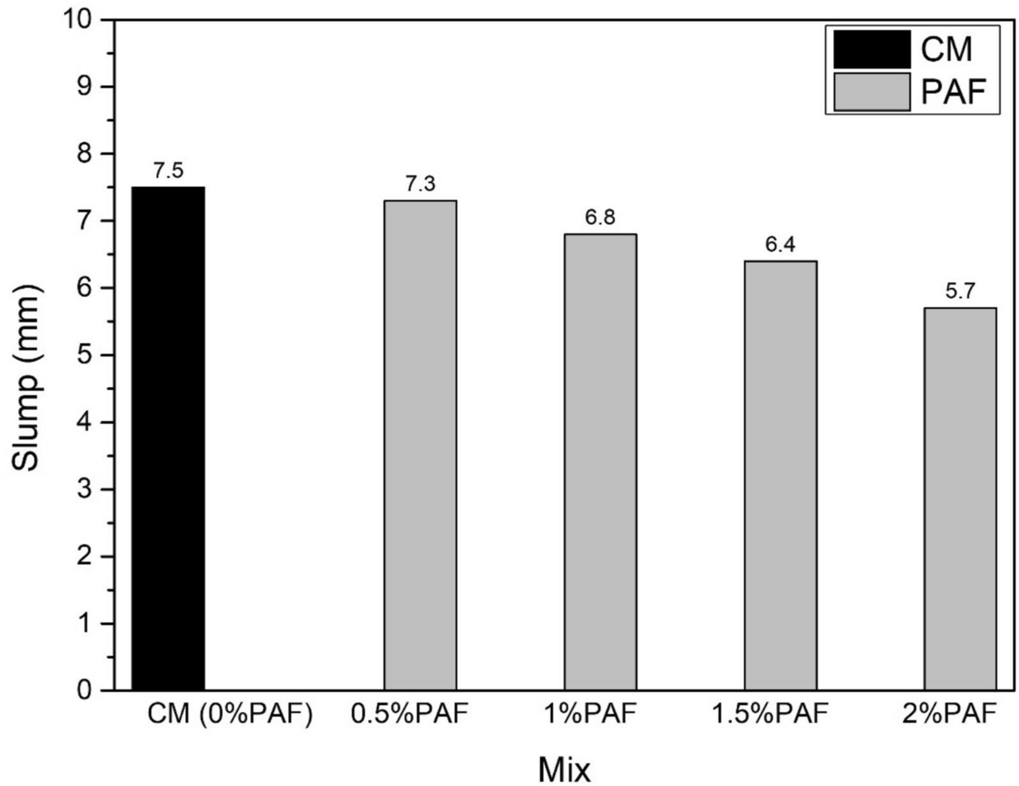

Fig. 4 Average slump values of concrete mixes with varying PAF contents

fibre degradation. PA0 (7.78%) had the highest loss, while mixes with PAF especially PA1.5% and PA2% exhibited lower values (5.39% and 5.54%, respectively), indicating that fibre inclusion may help reduce thermal decomposition and moisture escape at this temperature. These results are consistent with those of concrete incorporating Spanish broom and hemp fibres reported by (Juradin et al., 2021; Netinger Grubeša et al., 2018).

At 600 °C, the trend continued with further increases in mass loss, though at a slower rate. Again, PA0 had the highest loss (9.26%), while fibre-reinforced mixes such as PA1.5% (6.66%) and PA2% (6.18%) showed improved thermal stability. Overall, the inclusion of PAF reduced mass loss at higher temperatures, particularly at 400 °C and 600 °C, likely due to their contribution to matrix densification and delayed thermal degradation.

3.2.2 Compressive Strength

The compressive strength of concrete mixes incorporating different volume fractions of Phragmites australis fibres (PAF) was evaluated after exposure to elevated temperatures of 200 °C, 400 °C, and 600 °C, in addition to ambient conditions (23 °C), as shown in Fig. 6. The results reveal clear trends in the thermal degradation of concrete with varying fibre contents. At ambient temperature (23 °C), the control mix (PA0) without fibres exhibited the highest compressive strength at 43 MPa. As fibre content increased, the strength declined progressively. The 0.5% PAF mix maintained a relatively high value of 39 MPa, while the 1% mix reached 36 MPa. However, the compressive strength dropped more notably in mixes with 1.5% and 2% fibre content, reaching 28 MPa and 25 MPa, respectively. This reduction is likely due to the challenges associated with fibre dispersion, such as agglomeration and increased porosity, which can adversely affect the concrete's internal matrix.

Following exposure to 200 °C, a general decrease in compressive strength was observed across all mixes (Fig. 6). The control mix (PA0) showed a slight reduction to 41 MPa, retaining approximately 95% of its original strength, suggesting good thermal stability at this moderate temperature. Mixes containing fibres exhibited a more noticeable drop: the 0.5% and 1% PAF mixes reduced to 33 MPa and 31 MPa, respectively. In contrast, the 1.5% and 2% mixes showed lower values of 26 MPa and 23 MPa. While these fibre-reinforced mixes still retained reasonable strength, the data suggest that moderate fibre inclusion (0.5–1%) may be optimal for maintaining mechanical integrity under moderate thermal exposure.

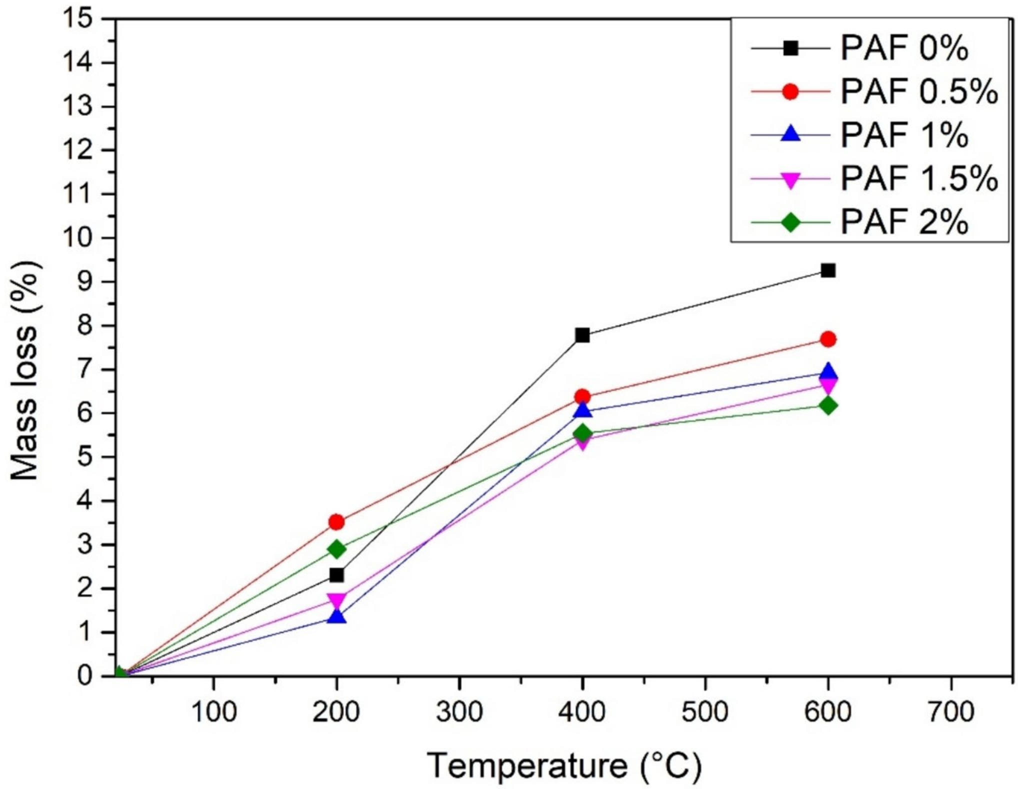

Fig. 5 Average mass loss of concrete mixes with different PAF contents after exposure to 200–600 °C

At 400 °C, the extent of thermal degradation became more pronounced. The control mix dropped further to 37 MPa, indicating a 14% loss from its ambient value. The fibre-reinforced mixes experienced greater reductions, particularly the 0.5% and 1% mixes, which converged at approximately 27–28 MPa. The 1.5% and 2% mixes decreased further to 22 MPa and 20 MPa, respectively. These findings reinforce the notion that fibre content beyond 1% can lead to accelerated matrix deterioration under elevated temperatures, likely due to increased microcracking and poor compaction associated with higher fibre volumes. This is consistent with the findings reported by (Netinger Grubeša et al., 2018) on hemp fibres within the same temperature range.

When exposed to 600 °C, all mixes experienced significant strength loss. The control mix reduced to 27 MPa, indicating a 37% drop from its original strength. Fibre-reinforced mixes were more affected, particularly at higher fibre volumes. The 0.5% PAF mix retained the highest residual strength among fibre mixes at 24 MPa, while the 2% PAF mix dropped drastically to 13 MPa. The trend suggests that although small quantities of PAF may offer some resistance to thermal cracking and spalling, excessive fibre content likely promotes charring, internal void formation, and structural weakening of the matrix under high-temperature exposure.

To better compare the performance trends, compressive strengths were normalized against their respective ambient values (see Fig. 7). The control mix without fibres (PA0) retained the highest proportion of its original strength at all temperature levels. At 200 °C, PA0 retained approximately 95.3% of its ambient strength, while further degradation occurred at 400 °C and 600 °C, dropping to 86.0% and 62.8%, respectively. This steady decline reflects the expected thermal degradation of unreinforced concrete but indicates relatively stable performance compared to fibre-reinforced mixes.

Among the PAF-reinforced concretes, the results at 200 °C revealed that mixes with 1.5% and 2% fibre content exhibited slightly higher residual strength (92.9% and 92.0%, respectively) than the mixes with 0.5% and 1% fibres (84.6% and 86.1%). This trend may suggest that at moderate heating, higher fibre contents initially contribute positively by enhancing the matrix's crack-bridging capacity and reducing thermal microcracking.

However, at 400 °C, the performance of the fibre-reinforced mixes declined more noticeably. The PA0.5% mix showed the largest reduction, retaining only 69.2% of its original strength, while the PA2% mix performed slightly

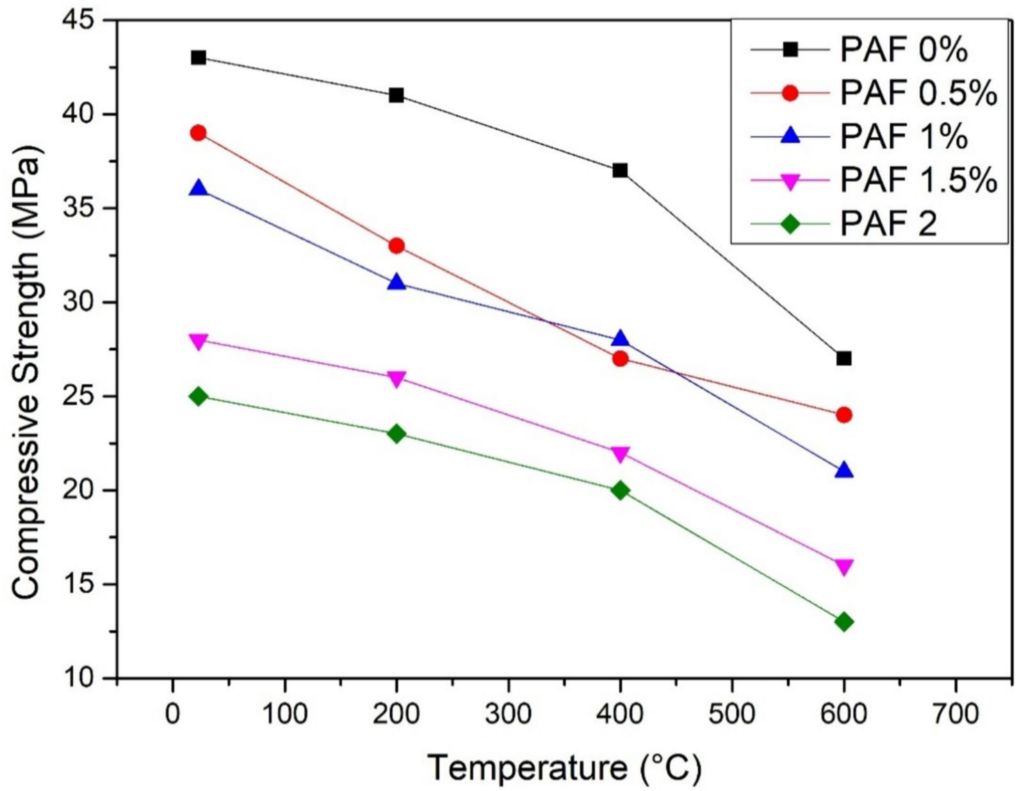

Fig. 6 Average compressive strength of concrete mixes with varying volumes of (PAF) after exposure to elevated temperatures

better, maintaining 80% of its strength. Mixes with 1% and 1.5% fibres fell in between, retaining 77.8% and 78.6% of their initial strength, respectively. At 600 °C, a considerable reduction in strength was observed across all mixes. The control mix retained 62.8% of its original strength, outperforming all fibre-containing mixes. The lowest residual strength was recorded for the PA2% mix at 52%, followed by PA1.5% at 57.1%. Interestingly, moderate fibre dosages (0.5% and 1%) performed comparatively better under this extreme condition, with residual strengths of 61.5% and 58.3%, respectively. These observations are consistent with the findings reported) for specimens reinforced with a hybrid combination of jute and sisal with steel fibres.

3.2.3 Splitting Tensile Strength

The splitting tensile strength of concrete mixes incorporating different volume fractions of Phragmites australis fibres (PAF) was evaluated under ambient conditions and after exposure to 200 °C, 400 °C, and 600 °C, as shown in Fig. 8. At ambient temperature (23 °C), the control mix (PA0) achieved a tensile strength of 2.81 MPa. Interestingly, the mix containing 0.5% PAF outperformed all others with a strength of 2.94 MPa, suggesting that a small addition of fibres enhances crack-bridging capacity and resists splitting failure. However, as fibre content increased beyond 0.5%, tensile strength declined progressively to 2.52 MPa (PA1%), 2.45 MPa (PA1.5%), and 2.03 MPa (PA2%). This reduction is likely due to fibre clumping, poor dispersion, and weak fibre–matrix bonding at higher fibre volumes.

At 200 °C, all mixes showed only a slight decrease in tensile strength. The control mix dropped marginally to 2.75 MPa (a 2.1% reduction), while the PAF mixes showed a consistent but mild decrease, maintaining tensile strengths of 2.82 MPa (PA0.5%), 2.42 MPa (PA1%), 2.41 MPa (PA1.5%), and 1.95 MPa (PA2%). These results suggest that PAF-reinforced mixes, especially those with lower fibre content, retain tensile strength effectively under moderate thermal exposure.

Upon exposure to 400 °C, the strength degradation became more evident. The control mix declined to 2.61 MPa, while PA0.5% showed better retention with a value of 2.75 MPa. In contrast, mixes with 1%, 1.5%, and 2% PAF dropped to 2.10 MPa, 1.98 MPa, and 1.64 MPa, respectively. These results reflect that higher fibre content may not contribute positively to tensile capacity under sustained thermal stress due to degradation of organic fibres, loss of interfacial adhesion, and increased porosity.

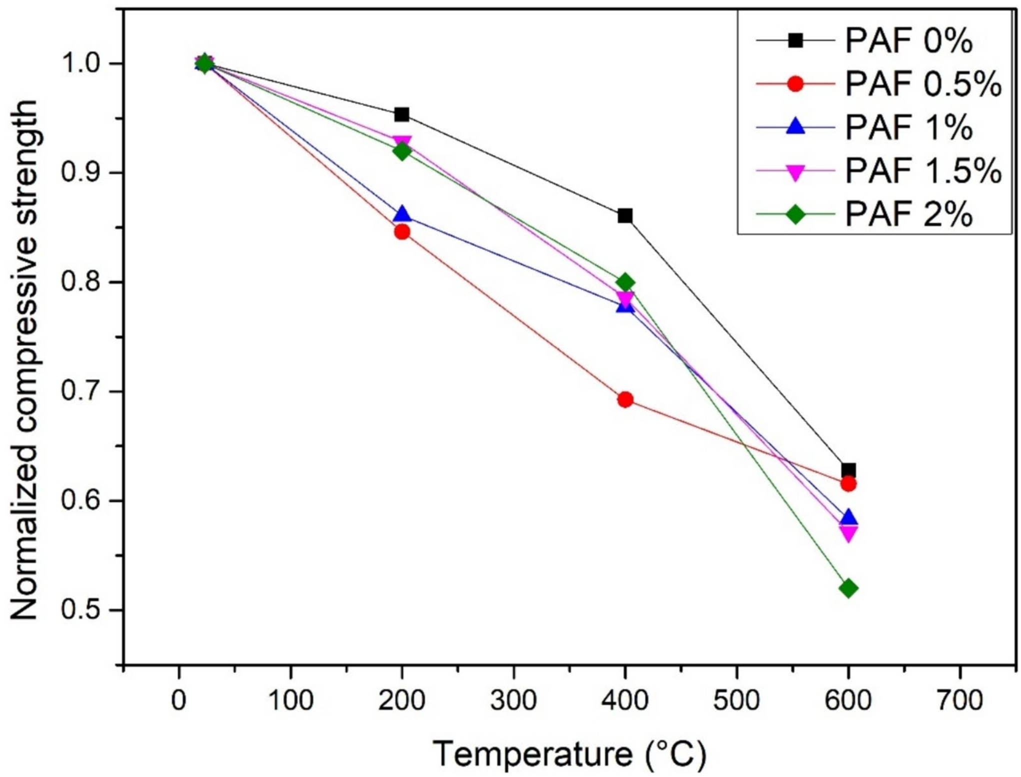

Fig. 7 Normalized compressive strength retention of PAF-reinforced concrete relative to ambient conditions after heating

At 600 °C, all mixes experienced significant deterioration in tensile strength. The control mix retained only 1.35 MPa, a 52% loss from its original strength. Similarly, the PAF mixes recorded 1.56 MPa (PA0.5%), 1.25 MPa (PA1%), 1.22 MPa (PA1.5%), and 1.11 MPa (PA2%). Despite the overall reduction, the 0.5% PAF mix demonstrated the highest residual strength among all, maintaining approximately 53% of its initial value which slightly higher than even the control. This may be attributed to fibre bridging and microcrack confinement at this moderate dosage, which helped preserve internal integrity under heat (Fig. 9).

When the tensile strength results were normalized relative to their respective ambient values, a similar trend was observed (Fig. 10). At 600 °C, the PA0.5% mix exhibited the highest normalized strength (0.53), followed by PA2% (0.55), PA1% (0.50), PA1.5% (0.50), and the control mix (0.48). These findings indicate that at extreme temperatures, small fibre inclusions (particularly 0.5%) may aid in mitigating the adverse effects of thermal exposure on tensile behaviour, while excessive fibre volumes offer no additional benefit and may even accelerate degradation. Pineapple fibres exhibited a similar trend, with tensile strength gradually decreasing as the temperature increased. The reduction was modest up to 400 °C, but a sharp decline of approximately 75% was observed at 600 °C (Mathew & Paul, 2017).

The post-test surface examination of cylindrical concrete specimens reinforced with Phragmites australis fibres (PAF) revealed distinct changes in crack patterns, fibre distribution, pull-out behaviour, and surface coloration with increasing exposure temperatures as shown in Fig. 11. These visual cues offer valuable insights into the thermal degradation process and the role of fibres in resisting splitting failure under elevated temperatures.

At 200 °C, all specimens maintained relatively uniform surfaces with visible fibre pull-out, particularly in mixes containing 0.5% and 1.0% fibres. The fibre distribution appeared uniform, and some fibres were still clearly embedded across the crack planes, indicating strong mechanical interlock and effective stress transfer. The surface colour remained light grey with minimal discoloration, and the cracks were narrow and primarily vertical. Fibre bridging was evident, particularly in the PA0.5 and PA1.0 mixes, which helped control crack width and delayed macro-crack formation.

At 400 °C, the surface colour began to shift toward a light red, indicating the onset of thermal degradation of the cement matrix and organic components of the fibres. Fibre pull-out marks were more pronounced, especially

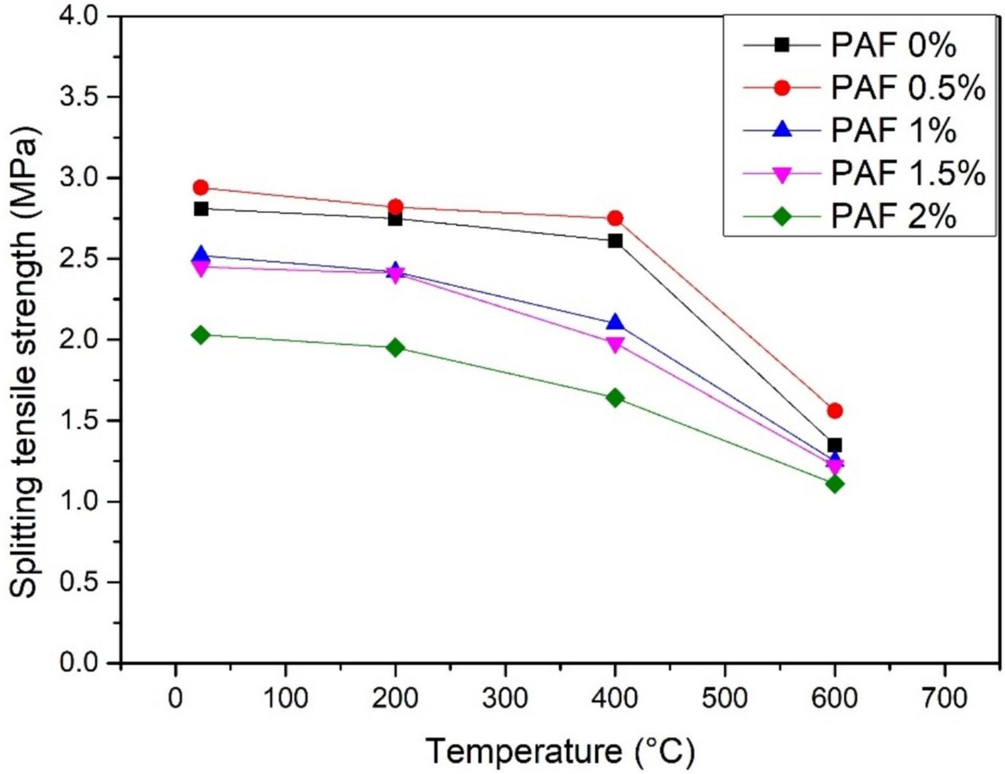

Fig. 8 Average splitting tensile strength of PAF-reinforced concrete at ambient and elevated temperatures

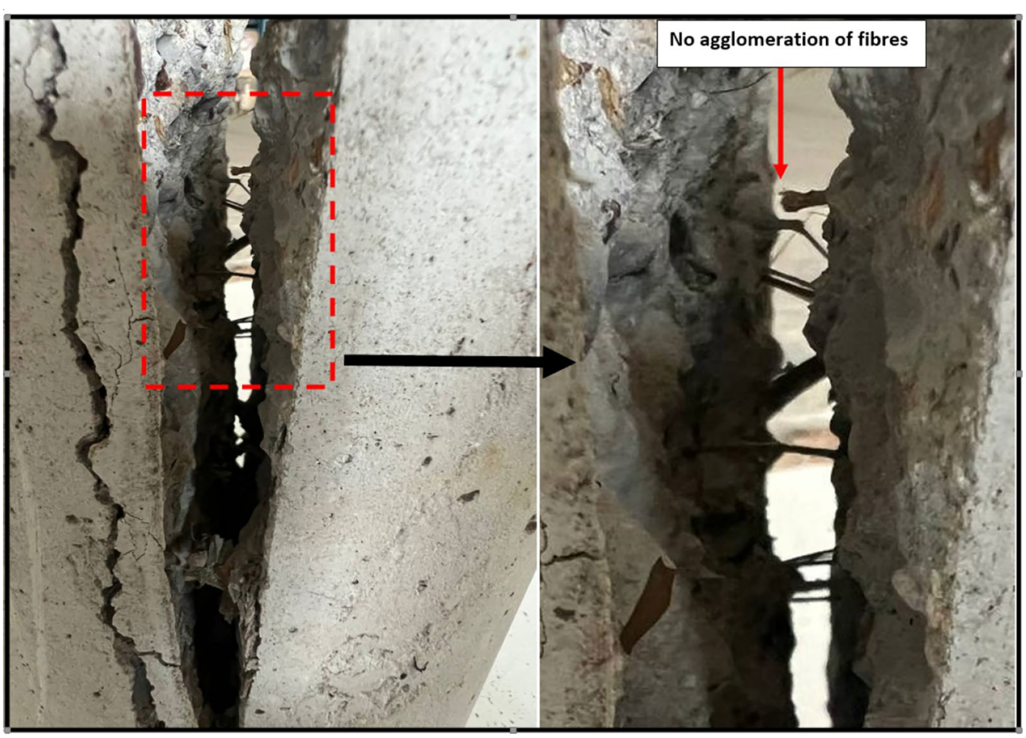

Fig. 9 No agglomeration of PAF at (0.5%), indicating uniform fibre dispersion within the mix

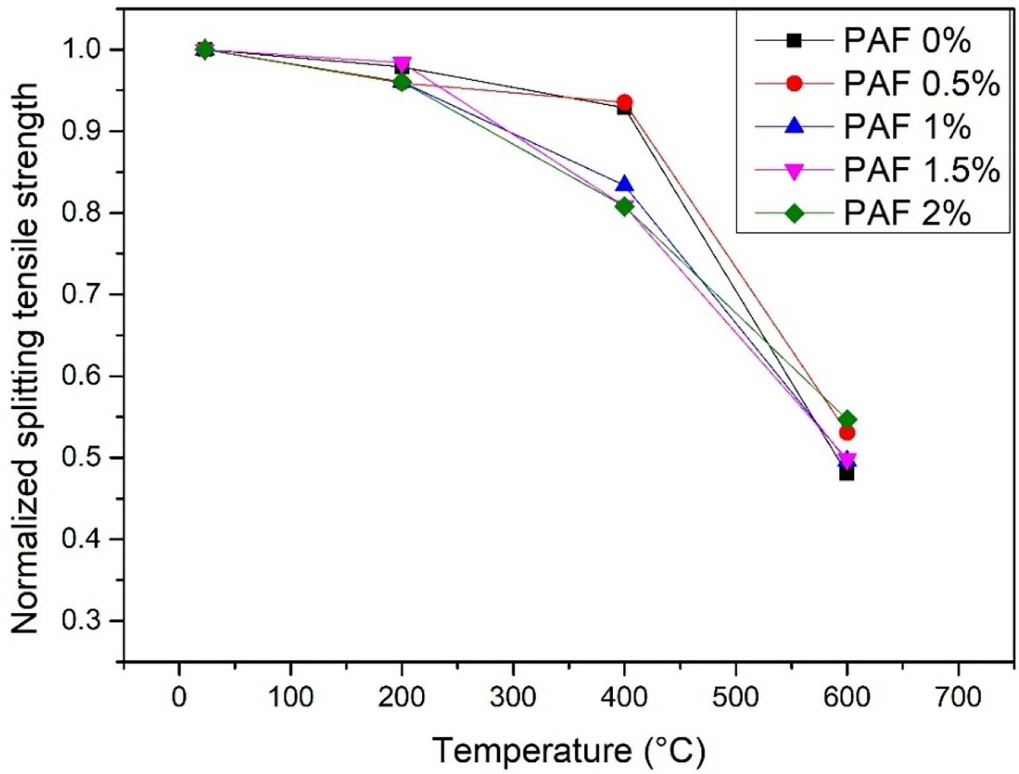

Fig.10 Normalized splitting tensile strength of concrete mixes containing PAF at different temperatures

in the PA1.5 and PA2.0 mixes, suggesting fibre–matrix bond weakening. The distribution of fibres became less uniform at higher dosages, with visible clustering in the PA2.0 mix (see Fig. 11). Cracks widened and began to branch, but some residual fibre bridging was still apparent, particularly in the lower fibre content mixes. The fibres themselves started to lose their natural colour, showing signs of partial colour change.

At 600 °C, the surfaces exhibited remarkable deterioration. A light to dark red colouration was observed across all fibre-reinforced mixes, indicating substantial carbonization and thermal decomposition of the fibres. The cracks became wider, deeper, and more irregular, extending radially in some cases. Fibre remnants were mostly charred, and pull-out was minimal, indicating that the fibres had largely lost their structural contribution. In mixes with higher fibre content (PA1.5 and PA2.0), fibre clumping and poor dispersion became evident (see Fig. 12), which contributed to uneven crack development and localized matrix degradation. Surface scaling and delamination were also visible, particularly in the PA2.0 mix, reflecting internal steam pressure and loss of cohesion.

3.2.4 Flexural Strength

The flexural strength of concrete mixes with varying contents of Phragmites australis fibres (PAF) was assessed under ambient conditions and after thermal exposure to 200 °C, 400 °C, and 600 °C (see Fig. 13). At ambient temperature (23 °C), the control mix (PA0) achieved a flexural strength of 7.85 MPa. The addition of 0.5% PAF resulted in a substantial increase to 9.65 MPa representing the peak performance among all mixes. This enhancement is attributed to effective fibre bridging across cracks and the improved energy absorption capacity introduced by low fibre content. The 1% and 1.5% mixes also showed good strength (9.05 MPa and 8.22 MPa, respectively), while the 2% PAF mix recorded a significant drop to 6.10 MPa, likely due to poor workability, fibre clumping, and entrapped air that reduced structural integrity which is similar to what observed in Fig. 12.

At 200 °C, the reduction in flexural strength was modest for all mixes. The control mix declined slightly to 7.65 MPa, while the 0.5% PAF mix retained 8.99 MPa. Similarly, the 1% and 1.5% mixes recorded strengths of 8.66 MPa and 8.01 MPa, respectively. The 2% PAF mix dropped slightly to 5.89 MPa. These results show that fibre-reinforced concrete, particularly at 0.5–1% content, maintains high crack resistance under mild thermal

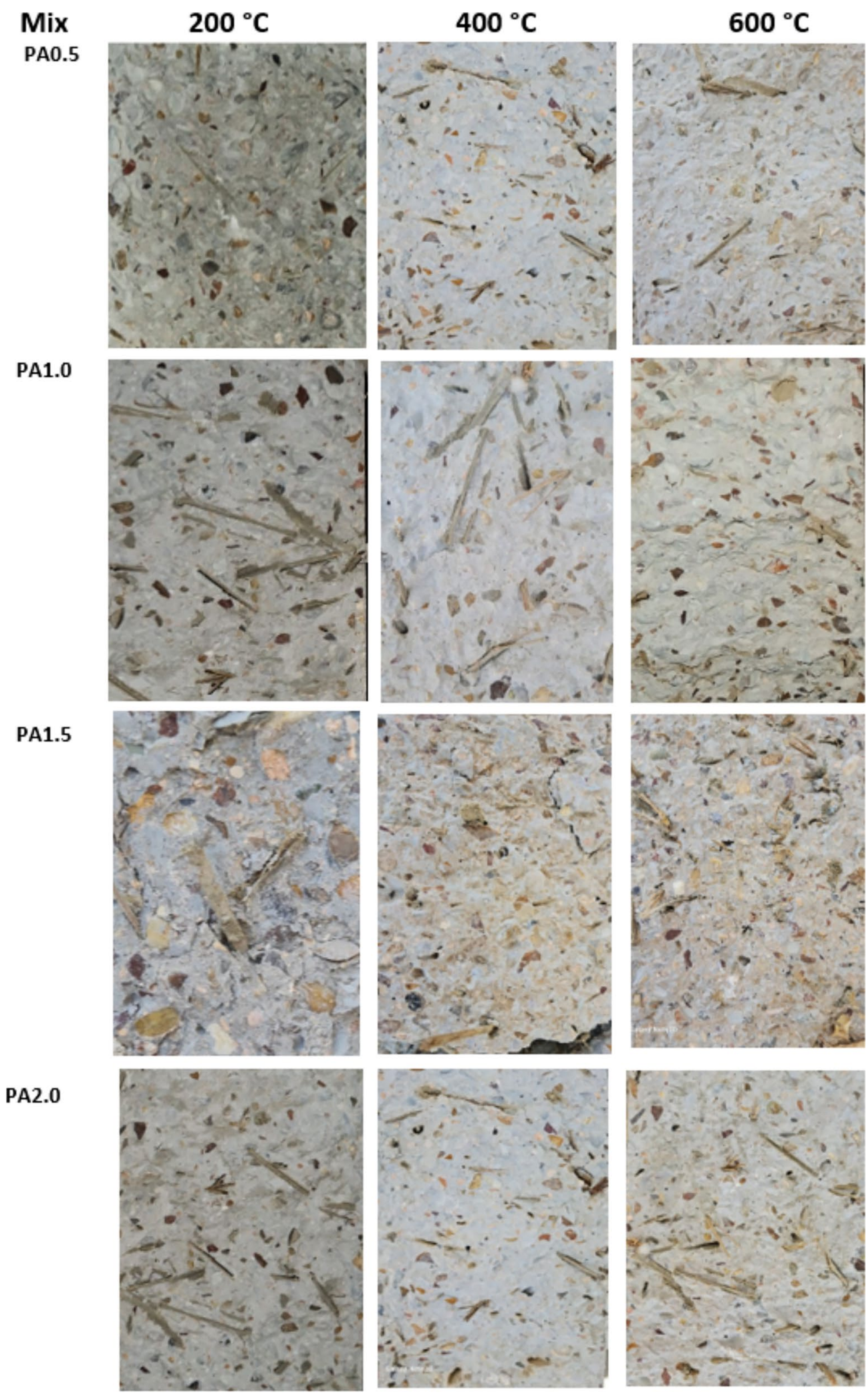

Fig. 11 Post-test surfaces showing crack patterns, fibre pull-out, and colour changes in PAF-reinforced concrete at 200–600 °C

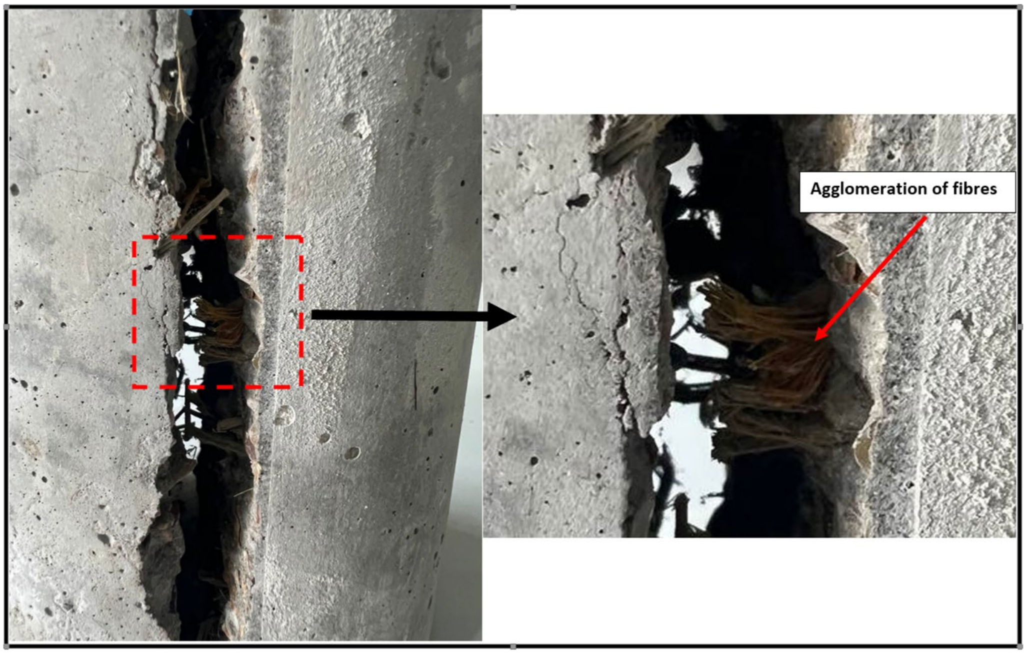

Fig. 12 Fibre's clustering observed at higher PAF content (2%), indicating poor dispersion

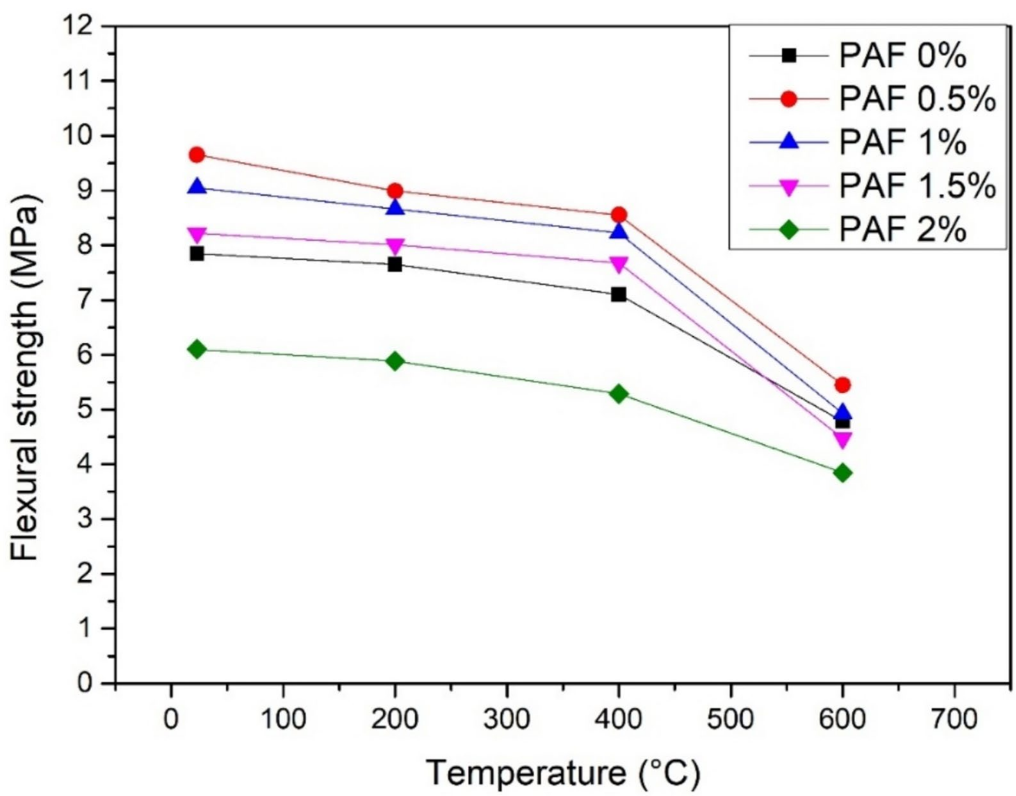

Fig. 13 Average flexural strength performance of concrete containing Phragmites australis fibres subjected to elevated exposure

exposure. The fibre's bridging action seems to remain effective at this temperature, delaying crack propagation and reducing the rate of strength deterioration.

When the temperature increased to 400 °C, further reductions were observed. The control mix decreased to 7.10 MPa, while the 0.5% and 1% mixes recorded 8.55 MPa and 8.23 MPa, respectively. Mixes with higher fibre content (1.5% and 2%) dropped to 7.68 MPa and 5.29 MPa, respectively. Although a downward trend was evident, the residual flexural strength remained relatively high for 0.5–1% mixes, suggesting that these fibre volumes can still contribute effectively to flexural toughness even at elevated thermal stress levels.

At 600 °C, all mixes showed marked deterioration in flexural strength. The control mix decreased to 4.78 MPa, indicating a 39% reduction. The 0.5% PAF mix dropped to 5.45 MPa, while the 1% and 1.5% mixes recorded 4.93 MPa and 4.47 MPa, respectively. Interestingly, the 2% PAF mix, although initially the weakest, retained 3.85 MPa, which translates to a slightly higher normalized retention (63%) than other mixes at this temperature. This may reflect the insulating effect of densely packed fibres that, despite reducing initial strength, may help retard heat penetration and delay degradation of the cement matrix. Nevertheless, the absolute values confirm that lower fibre dosages still perform better under combined mechanical and thermal stresses. A similar trend was observed with coir fibres, as reported by (Othuman Mydin et al., 2019).

Normalized flexural strength values reinforce this trend (Fig. 14). At 200 °C and 400 °C, mixes with 0.5% and 1% fibres retained more than 88% of their original flexural strength. However, beyond 400 °C, all mixes experienced significant degradation, with the control mix retaining 60.9% of its original value and the fibre-reinforced mixes ranging from 54.4% to 63.1%. The 2% PAF mix showed unexpectedly higher relative retention at 600 °C, though it still remained the weakest in absolute strength. These results align with those reported for the combination of micro straight steel fibres (MSS), macro hooked-end steel fibres (MHS), and micro jute fibres (MJ) as reported by (Ridha, 2024).

3.2.5 Ultrasonic Pulse Velocity (UPV)

The UPV test results provide insight into the internal integrity and homogeneity of concrete after exposure to elevated temperatures. At ambient temperature (23 °C), the control mix (PAF0%) exhibited the highest pulse velocity of 4.65 km/s, indicating excellent compactness

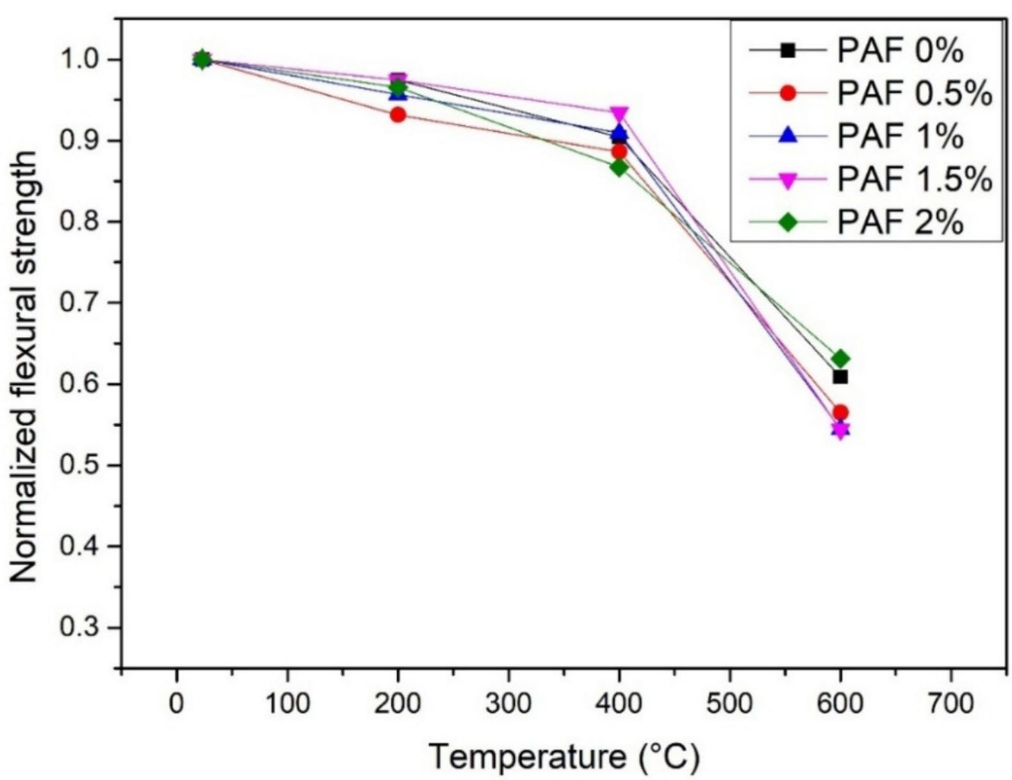

Fig. 14 Normalized flexural strength of concrete incorporating PAF fibres exposed to elevated temperatures

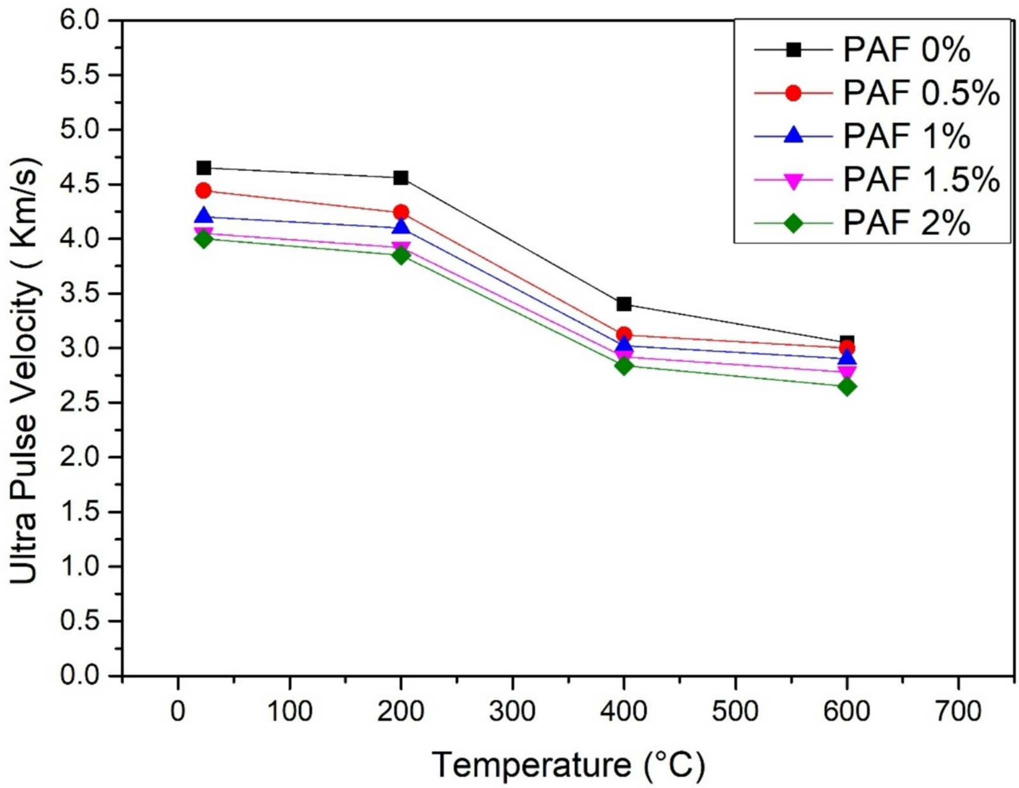

Fig. 15 Average ultrasonic Pulse Velocity (UPV) test results for PAF-reinforced concrete after heating to different temperature levels

and continuity of the concrete matrix (see Fig. 15). As PAF content increased, a gradual decline in UPV values was observed dropping to 4.44 km/s for 0.5% PAF, 4.20 km/s for 1% PAF, and reaching 4.00 km/s at 2% PAF. This decline suggests that the incorporation of fibres slightly disrupted the internal matrix continuity, possibly due to fibre clustering and entrapped air, especially at higher fibre volumes.

After exposure to 200 °C, all mixes showed a minor reduction in UPV, consistent with early stage microcracking and matrix dehydration. The control mix dropped slightly to 4.56 km/s, while fibre-reinforced mixes ranged from 4.24 km/s (0.5% PAF) to 3.85 km/s (2% PAF). The relatively moderate decrease at this stage indicates that the structural network remained largely intact, particularly for low fibre dosages.

At 400 °C, a more pronounced decline in UPV was observed across all mixes. The control mix dropped to 3.40 km/s, and mixes with PAF saw values between 3.12 km/s (0.5% PAF) and 2.84 km/s (2% PAF). This suggests significant internal cracking, increased porosity, and possible fibre degradation, leading to acoustic discontinuities within the matrix. Notably, mixes with higher fibre content (1.5% and 2%) showed sharper reductions, reflecting poorer heat resistance and increased matrix deterioration.

At 600 °C, UPV values reached their lowest for all mixes, with the control mix recording 3.05 km/s and the 2% PAF mix falling to just 2.65 km/s. These low values indicate substantial microstructural damage, likely caused by intense thermal stresses, fibre charring, and breakdown of the cementitious bonds. The decrease in UPV was more severe in fibre-reinforced mixes compared to the control, which may reflect additional porosity introduced by the burned-out organic fibres and disrupted matrix–fibre interfacial zones.

Overall, UPV test results reveal that while PAF can enhance certain mechanical properties, higher fibre contents ($\geq$1.5%) may compromise the internal quality of concrete, particularly after exposure to high temperatures. The results also highlight the importance of optimizing fibre volume to balance strength and durability without sacrificing matrix integrity. The declining UPV trend with increasing temperature confirms that thermal exposure induces progressive microstructural degradation in both plain and fibre-reinforced concretes.

3.3 Regression Analysis of Normalized Residual Strengths

To quantify the degradation in mechanical properties of Phragmites australis fibre-reinforced concrete (PAFRC) after exposure to elevated temperatures, linear regression models were developed for the normalized residual strengths (i.e., the ratio of residual to original strength) of compressive strength $\left(\frac{f_c}{f_c'}\right)$, splitting tensile strength $\left(\frac{f_t}{f_t'}\right)$, and flexural strength $\left(\frac{f_f}{f_f'}\right)$. The normalized values were plotted against temperature, and best-fit linear equations were generated for each fibre content (0–2%) (Figs. 16, 17, 18). These regression models provide simplified predictive tools to estimate the remaining mechanical performance of the concrete as a function of temperature. To evaluate the thermal degradation behaviour of Phragmites australis fibre-reinforced concrete (PAFRC), linear regression models were developed to relate the normalized residual mechanical strengths compressive $\left(\frac{f_c}{f_c'}\right)$, splitting tensile $\left(\frac{f_t}{f_t'}\right)$, and flexural strength $\left(\frac{f_f}{f_f'}\right)$ to exposure temperature. Normalized strength values were plotted as a function of temperature for all fibre contents (0–2%), and best-fit linear equations were obtained (Figs. 16, 17, 18). These models provide practical predictive relationships for estimating the retained mechanical performance of PAFRC subjected to temperatures between 23 °C and 600 °C. The general form of the regression expression is:

$$\frac{f}{f'} = a - b\left(\frac{T}{1000}\right), 23^\circ\mathrm{C} \leq T \leq 600^\circ\mathrm{C} \tag{1}$$

where:

- f/f' is the normalized strength (compressive, tensile, or flexural),
- T is the exposure temperature in degrees Celsius,
- a and b are regression coefficients derived from empirical data,
- R^2 is the coefficient of determination indicating the goodness of fit.

3.3.1 *Compressive Strength*

The compressive strength data revealed that the strength degradation with increasing temperature followed a linear trend for all mixes. The control mix (PA0) exhibited the steepest slope, indicating greater sensitivity to temperature rise. As fibre content increased, the intercepts

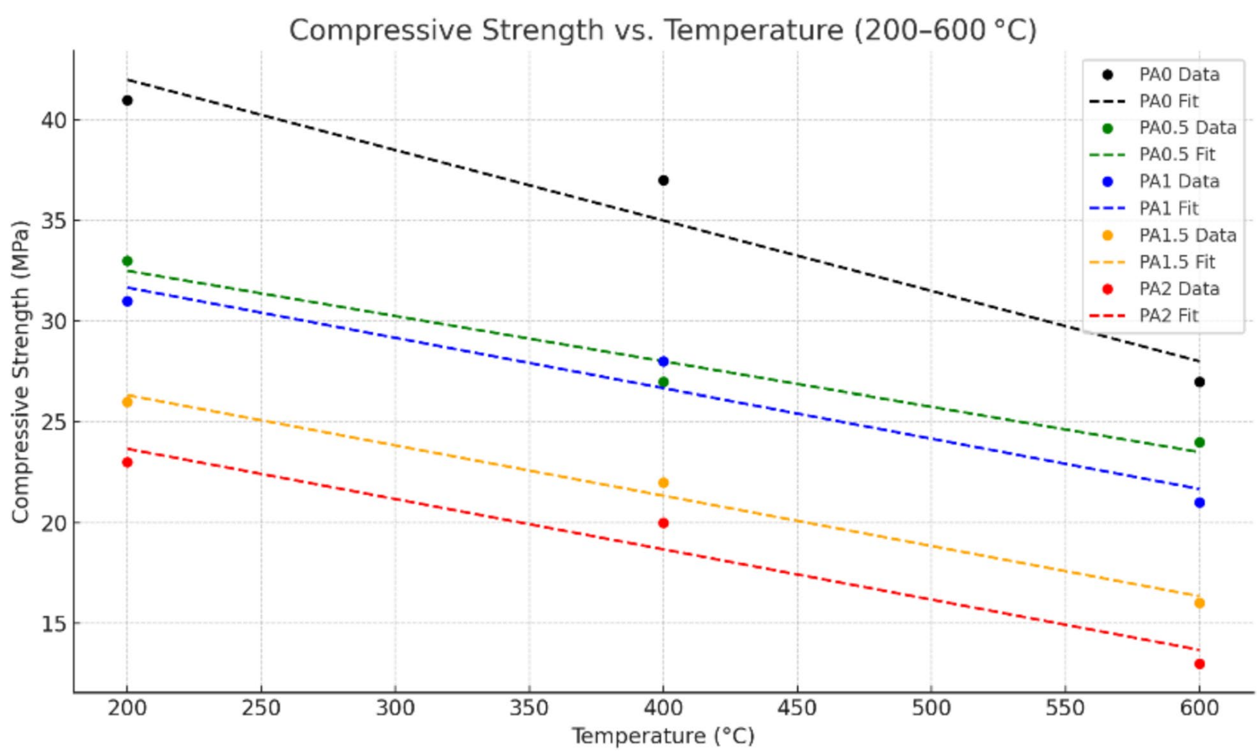

Fig. 16 Compressive strength vs. temperature (200–600 °C) for mixes with varying PAF content. Linear trends show strength loss with increasing temperature

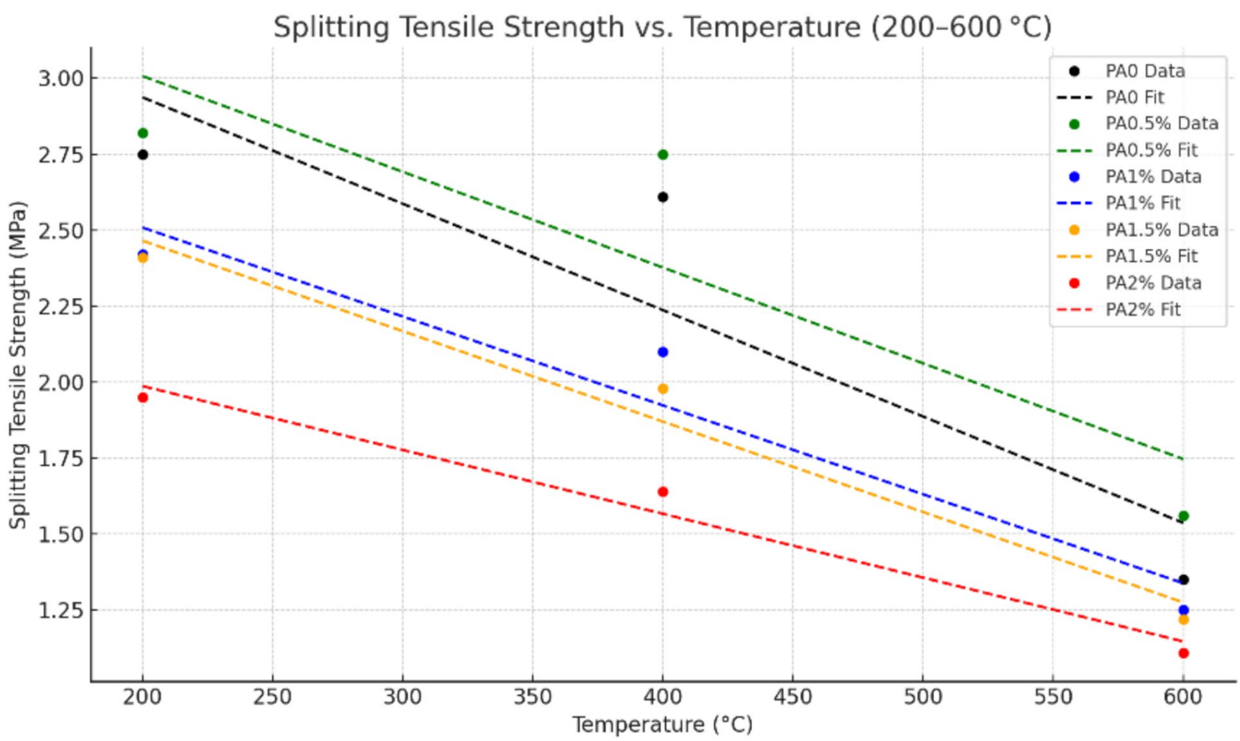

Fig. 17 Splitting tensile strength vs. temperature (200–600 °C) for different PAF mixes. Moderate fibre content retained higher strength as temperature increased

also increased slightly, suggesting enhanced residual strength at ambient temperature due to fibre inclusion. However, the negative slope coefficients imply that degradation rates accelerated at higher dosages, likely due to poor dispersion or fibre agglomeration.

For example, the normalized compressive strength of PA0.5% concrete can be estimated using:

$$\frac{f_c}{f_c'} = 0.95 - 0.58\left(\frac{T}{1000}\right), 23^\circ C \le T \le 600^\circ C, R^2 = 0.96 \quad (2)$$

This model suggests that at 400 °C, approximately 72% of the original strength is retained.

3.3.2 Splitting Tensile Strength

Normalized tensile strength also followed a linear decreasing trend with temperature, with higher fibre contents generally exhibiting stronger correlations (higher R^2). Fibre reinforcement provided notable improvement in tensile retention up to 400 °C due to enhanced crack bridging and energy absorption mechanisms. The PA1.5% mix demonstrated the most favourable thermal performance, with degradation initiating more gradually than in lower dosage mixtures. The corresponding regression model is:

$$\frac{f_t}{f_t'} = 1.25 - 1.21\left(\frac{T}{1000}\right), 23^\circ C \le T \le 600^\circ C, R^2 = 0.98 \quad (3)$$

This reflects a 20–25% loss of tensile strength at 400 °C, highlighting the fibre's crack-bridging role at moderate temperatures.

3.3.3 Flexural Strength

Flexural strength regression models revealed similar patterns to tensile strength. Fibre-reinforced mixes, especially PA1% and PA1.5%, showed higher initial normalized values and moderate degradation rates. However, above 400 °C, the deterioration became more pronounced, likely due to thermal decomposition of the fibres.

For example:

$$\frac{f_f}{f_f'} = 1.22 - 1.03\left(\frac{T}{1000}\right), 23^\circ C \le T \le 600^\circ C, R^2 = 0.84 \quad (4)$$

The PA2% mix showed slightly lower retention and a flatter slope, possibly due to poor workability and fibre clumping. These regression equations are valuable tools for predicting performance degradation in structural applications, where exposure to high temperatures is a concern (Table 2). They can support fire resistance

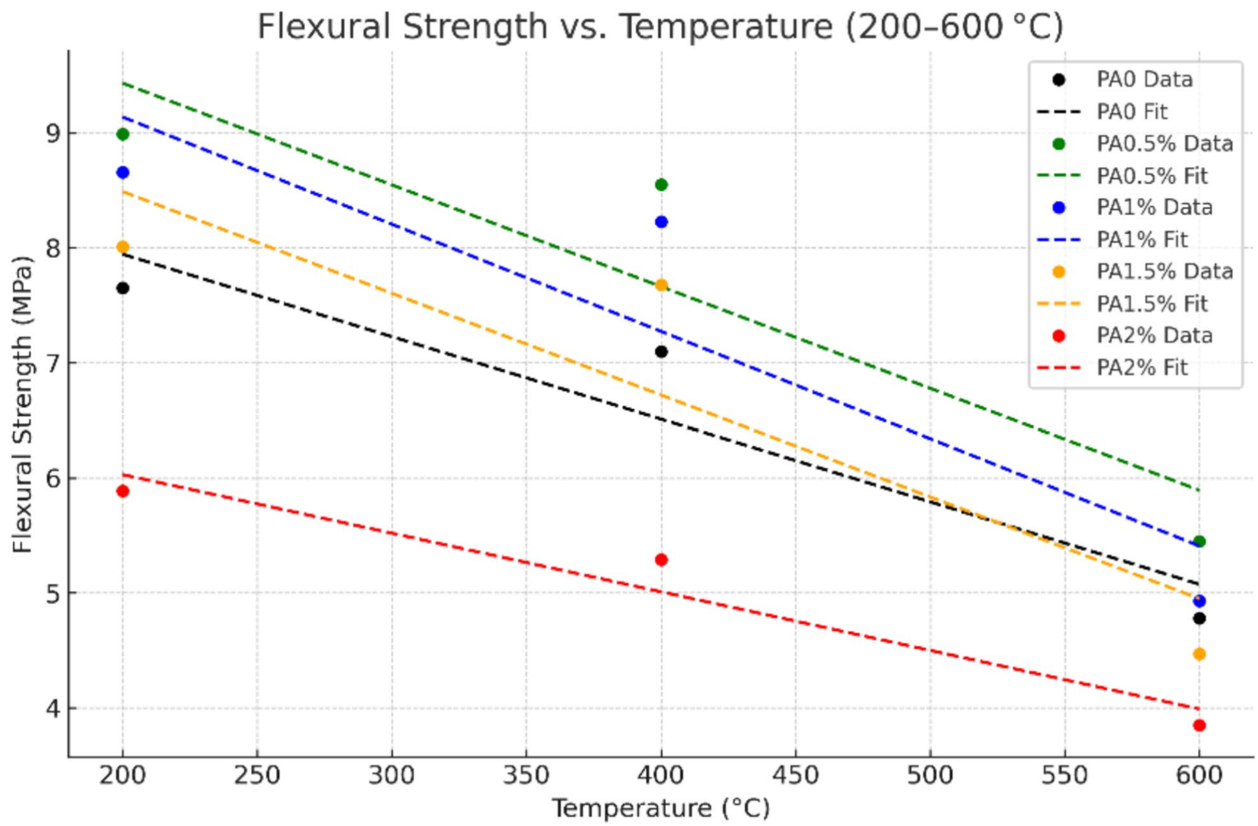

Fig. 18 Flexural strength vs. temperature (200–600 °C) for PAF-reinforced mixes. Strength decreased with temperature; 0.5–1% fibres showed better retention at lower temperatures

design, post-fire assessment, and structural integrity evaluations. The relatively high R^2 values for most mixes confirm that linear models are appropriate for the studied temperature range (23 °C to 600 °C). However, it is important to note that beyond 600 °C, non-linear degradation mechanisms may dominate, and these linear models may no longer hold.

Figure 16 depicts the degradation trend (linear regression fits) of compressive strength in concrete mixes containing 0–2% *Phragmites australis* fibres when exposed to elevated temperatures between 200 °C and 600 °C. All mixes showed a progressive reduction in compressive strength with increasing temperature. The control mix (PA0) exhibited the highest thermal resistance, while mixes with higher fibre contents (especially PA2%) displayed steeper declines. The linear regression lines effectively illustrate the thermal sensitivity of each mix, indicating that excessive fibre addition may accelerate strength deterioration under heat due to fibre degradation and microstructural disruption.

Figure 17 shows the variation in splitting tensile strength of concrete reinforced with different volumes of Phragmites australis fibres subjected to high temperatures. The general trend reveals a decrease in tensile strength as temperature increases. At 200 °C and 400 °C, mixes with 0.5% and 1.0% fibres retained more tensile strength compared to other mixes, suggesting enhanced fibre-bridging and bond interaction. However, all mixes experienced significant strength loss at 600 °C. The regression lines highlight the rate of tensile degradation, with higher fibre dosages (1.5% and 2%) showing greater thermal vulnerability.

Figure 18 illustrates the effect of elevated temperature on the flexural strength of concrete with varying contents of Phragmites australis fibres. Flexural performance generally decreased with rising temperature across all fibre dosages. At 200 °C and 400 °C, mixes with 0.5% and 1% fibres showed better flexural resistance due to effective crack-bridging. However, at 600 °C, fibre degradation became dominant, leading to significant strength reduction. The regression curves provide clear insight into the rate of thermal degradation, demonstrating that while moderate fibre addition enhances flexural strength at lower temperatures, higher dosages or extreme heating reduce performance due to poor fibre dispersion and carbonization.

Table 2 Regression equations for normalized residual strengths of concrete with PAF at 200–600 °C

Relative residual strength	Volume fraction (%)	Regression equations	R^2
Compressive strength	0	$\frac{f_c}{f'_c} = 1.14 - 0.81\left(\frac{T}{1000}\right), 23\ ^\circ\text{C} \leq T \leq 600\ ^\circ\text{C}$	0.94
	0.5	$\frac{f_c}{f'_c} = 0.95 - 0.58\left(\frac{T}{1000}\right), 23^\circ\text{C} \leq T \leq 600^\circ\text{C}$	0.96
	1	$\frac{f_c}{f'_c} = 1.02 - 0.69\left(\frac{T}{1000}\right), 23^\circ\text{C} \leq T \leq 600^\circ\text{C}$	0.95
	1.5	$\frac{f_c}{f'_c} = 1.12 - 0.89\left(\frac{T}{1000}\right), 23^\circ\text{C} \leq T \leq 600^\circ\text{C}$	0.99
	2	$\frac{f_c}{f'_c} = 0.95 - 0.58\left(\frac{T}{1000}\right), 23^\circ\text{C} \leq T \leq 600^\circ\text{C}$	0.95
Splitting tensile strength	0	$\frac{f_t}{f'_t} = 1.29 - 1.25\left(\frac{T}{1000}\right), 23^\circ\text{C} \leq T \leq 600^\circ\text{C}$	0.82
	0.5	$\frac{f_t}{f'_t} = 1.24 - 1.07\left(\frac{T}{1000}\right), 23^\circ\text{C} \leq T \leq 600^\circ\text{C}$	0.79
	1	$\frac{f_t}{f'_t} = 1.23 - 1.16\left(\frac{T}{1000}\right), 23^\circ\text{C} \leq T \leq 600^\circ\text{C}$	0.94
	1.5	$\frac{f_t}{f'_t} = 1.25 - 1.21\left(\frac{T}{1000}\right), 23^\circ\text{C} \leq T \leq 600^\circ\text{C}$	0.98
	2	$\frac{f_t}{f'_t} = 1.19 - 1.03\left(\frac{T}{1000}\right), 23^\circ\text{C} \leq T \leq 600^\circ\text{C}$	0.98
Flexural strength	0	$\frac{f_f}{f'_f} = 1.19 - 0.91\left(\frac{T}{1000}\right), 23^\circ\text{C} \leq T \leq 600^\circ\text{C}$	0.89
	0.5	$\frac{f_f}{f'_f} = 1.16 - 0.92\left(\frac{T}{1000}\right), 23^\circ\text{C} \leq T \leq 600^\circ\text{C}$	0.84
	1	$\frac{f_f}{f'_f} = 1.22 - 1.03\left(\frac{T}{1000}\right), 23^\circ\text{C} \leq T \leq 600^\circ\text{C}$	0.84
	1.5	$\frac{f_f}{f'_f} = 1.25 - 1.08\left(\frac{T}{1000}\right), 23^\circ\text{C} \leq T \leq 600^\circ\text{C}$	0.82
	2	$\frac{f_f}{f'_f} = 1.16 - 0.84\left(\frac{T}{1000}\right), 23^\circ\text{C} \leq T \leq 600^\circ\text{C}$	0.95

4 Conclusions

This study examined the incorporation of Phragmites australis fibres (PAF) into concrete and evaluated their effects on mechanical and ultrasonic properties after exposure to elevated temperatures (200 °C, 400 °C, and 600 °C). Based on the experimental results, the following conclusions are drawn:

- The inclusion of PAF reduced the slump of fresh concrete mixes due to the fibres' high surface area and water absorption capacity. However, acceptable workability was maintained up to a fibre content of 1%, beyond which a significant decrease in slump was observed.
- At ambient conditions, the addition of PAF particularly at 0.5–1%-resulted in marginal improvements in compressive strength. After thermal exposure, all mixes experienced strength degradation, with the most severe losses recorded at 600 °C. The control mix retained 62.8% of its initial strength at 600 °C, while PAF-reinforced mixes retained between 52% and 61%.
- Concrete reinforced with 0.5–1% PAF exhibited noticeable improvements in splitting tensile and flexural strength under ambient conditions. Post-heating performance demonstrated reduced strength across all mixes, yet PAF-reinforced specimens retained greater ductility and crack-bridging capacity, especially after exposure to 200 °C and 400 °C. At 600 °C, a drastic reduction (up to 75%) in tensile properties was observed, consistent with fibre degradation.
- UPV values decreased progressively with temperature, reflecting internal microcracking and material degradation. PAF-reinforced concretes displayed slightly lower UPV values compared to the control at all temperature levels, which may be attributed to the weaker fibre–matrix interface and increased porosity.
- PAF demonstrated the potential to enhance mechanical performance at ambient and moderately elevated temperatures. However, at 600 °C, thermal decomposition of the fibres led to substantial reductions in mechanical integrity.
- The optimal PAF content was found to be between 0.5% and 1%, providing a favourable balance between improved mechanical properties and acceptable workability. This range also showed the best post-heating performance relative to other dosages.

This study was limited to short-term mechanical and ultrasonic evaluations under controlled laboratory conditions. The long-term durability of PAF-reinforced concrete, including its resistance to cyclic thermal loading, moisture ingress, and chemical attack, remains unexplored. In addition, the variability in fibre morphology and distribution at higher dosages warrants further investigation. Future research should focus on optimizing fibre treatment methods, evaluating performance under real fire scenarios, and exploring hybrid reinforcement strategies that combine PA fibres with other sustainable or synthetic fibres to enhance thermal resilience and structural reliability.

Acknowledgements
The authors would like to express their sincere gratitude to the British Council UK for their valuable support in facilitating the studies presented in this paper.

Author contribution
Baydaa Hamdi Salih: Conceptualization, Formal analysis, Writing—original draft, Writing—review & editing. Sadoon Abdallah: Supervision, Writing—review & editing, Validation. Mohammed T. Nawar: Methodology, Investigation, Writing—review & editing. Ali J. Ali: Validation, Writing—review & editing. Mizi Fan: Methodology, Data curation Ameer A. Hilal: Visualization, Data curation, Writing—review & editing.

Funding
This research was supported by the British Council UK under the Research Environments grant (Grant No: RE-2023-129).

Availability of Data and Materials
All data generated or analyzed during this study are included in this published article.

Declarations

Ethics Approval and Consent to Participate
No competing interests exist in the submission of this manuscript, and manuscript is approved by all authors for publication.
The author declare that the work described was original research that has not been published previously, and not under consideration for publication elsewhere, in whole or in part.

Consent for Publication
Manuscript is approved by all authors for publication.

Competing Interest
The authors declare that they have no competing interest.

Received: 28 August 2025 Accepted: 1 December 2025
Published online: 31 December 2025

References

Abdalla, J. A., Hawileh, R. A., Bahurudeen, A., Jyothsna, G., Sofi, A., Shanmugam, V., & Thomas, B. S. (2023). A comprehensive review on the use of natural fibers in cement/geopolymer concrete: A step towards sustainability. *Case Studies in Construction Materials, 19*, Article e02244.

Abdallah, S., Salih, B. H., Mohammed, A. S., Fan, M., Hilal, A. A., Collins, P. E., & Sameer, J. O. (2025). Effect of alkali treatment on mechanical properties of concrete reinforced with phragmites australis fibres. *Asian Journal of Civil Engineering,* , 1–14. https://doi.org/10.1007/s42107-025-01556-9

Abdallah, S., Fan, M., & Cashell, K. A. (2017). Pull-out behaviour of straight and hooked-end steel fibres under elevated temperatures. *Cement and Concrete Research, 95*, 132–140. https://doi.org/10.1016/j.cemconres.2017.02.010

Alsaif, A., & Abbas, Y. M. (2025). Thermal stability and mechanical behavior of cementitious composites reinforced with industrial and recycled tire steel fibers under elevated temperature conditions. *Construction and Building Materials, 481*, Article 141580. https://doi.org/10.1016/j.conbuildmat.2025.141580

Altunişik, A. C., Akbulut, Y. E., Adanur, S., Günaydin, M., Mostofi, S., & Mosallam, A. (2023). Experimental study of the effect of different insulation schemes on fire performance of FRP strengthened concrete: FIRECOAT and REALROCK. *International Journal of Concrete Structures and Materials, 17*(1), 55.

Aluko, O. G., Yatim, J. M., Kadir, M. A. A., & Yahya, K. (2020). A review of properties of bio-fibrous concrete exposed to elevated temperatures. *Construction and Building Materials, 260*, Article 119671. https://doi.org/10.1016/j.conbuildmat.2020.119671

Amer, I., Kohail, M., El-Feky, M. S., Rashad, A., & Khalaf, M. A. (2023). Realistic evaluation of reinforcement bond strength in alkali-activated slag concrete exposed to elevated temperature. *International Journal of Concrete Structures and Materials, 17*(1), 36.

American Society for Testing and Materials. Committee C-9 on Concrete and Concrete Aggregates. (2011). *Standard test method for splitting tensile strength of cylindrical concrete specimens*. ASTM international.

Amin, M., Tayeh, B. A., & agwa, Is. (2020). Investigating the mechanical and microstructure properties of fibre-reinforced lightweight concrete under elevated temperatures. *Case Studies in Construction Materials, 13*, Article e00459. https://doi.org/10.1016/j.cscm.2020.e00459

Chen, L., Chen, Z., Xie, Z., Wei, L., Hua, J., Huang, L., & Yap, P. (2023). Recent developments on natural fiber concrete: A review of properties, sustainability, applications, barriers, and opportunities. *Developments in the Built Environment, 16*, Article 100255. https://doi.org/10.1016/j.dibe.2023.100255

Chun, Y., Ryu, E., Lee, Y., Kim, H., & Shin, Y. (2022). Experimental and analytical studies for the size effect on the axial strength of high-strength concrete walls with various fire-damaged areas. *International Journal of Concrete Structures and Materials, 16*(1), 32.

Dash, D., Mund, N. K., Upadhyay, D., Mishra, P., Dash, S. K., & Nayak, N. R. (2023). Evaluation of alkali and cellulose solvent pretreatments for fermentable sugar production from the biomass of *Phragmites karka* (Retz.) Trin. ex Steud.: A high biomass producing grass. *Biomass Conversion and Biorefinery, 13*(9), 7725–7736.

Durant, D., Farruggia, A., & Tricheur, A. (2020). Utilization of common reed (*Phragmites australis*) as bedding for housed suckler cows: Practical and economic aspects for farmers. *Resources, 9*(12), 140.

Elfaleh, I., Abbassi, F., Habibi, M., Ahmad, F., Guedri, M., Nasri, M., & Garnier, C. (2023). A comprehensive review of natural fibers and their composites: An eco-friendly alternative to conventional materials. *Results in Engineering, 19*, Article 101271. https://doi.org/10.1016/j.rineng.2023.101271

BS EN 12390-5. (2009). Testing hardened concrete. Flexural strength of test specimens. *British Standard Institution*

En, B. S. (2009). 12390-3, Testing hardened concrete-Part 3: Compressive strength of test specimens. *British Standards Institution*, p. 22

Eng, L., & Kim, C. (2025). Finite-element analysis of flexural strengthening performance of fire-damaged RC beams. *International Journal of Concrete Structures and Materials, 19*(1), 47.

Gencel, O., Nodehi, M., Yavuz Bayraktar, O., Kaplan, G., Benli, A., Gholampour, A., & Ozbakkaloglu, T. (2022). Basalt fiber-reinforced foam concrete containing silica fume: An experimental study. *Construction and Building Materials, 326*, Article 126861. https://doi.org/10.1016/j.conbuildmat.2022.126861

Han, H., Wang, Z., & Hadi Mosleh, M. (2024). High performance basalt-fibre modified cement for elevated temperature environments. *Construction and Building Materials, 448*, Article 138186. https://doi.org/10.1016/j.conbuildmat.2024.138186

Hung, C., Yulianti, E., & Agrawal, S. (2024). Microstructures, durability, and mechanical behavior of hybrid steel and PP fiber reinforced UHPC at elevated temperatures. *Construction and Building Materials, 447*, Article 138208. https://doi.org/10.1016/j.conbuildmat.2024.138208

Islam, M. S., & Ahmed, S. J. (2018). Influence of jute fiber on concrete properties. *Construction and Building Materials, 189*, 768–776. https://doi.org/10.1016/j.conbuildmat.2018.09.048

Juradin, S., Vranješ, L. K., Jozić, D., & Boko, I. (2021). Post-fire mechanical properties of concrete reinforced with spanish broom fibers. *Journal of Composites Science, 5*(10), 265.

Khatib, J. M., ElKhatib, L. W., Elkordi, A., & Sonebi, M. (2023). Length change of mortar containing Phragmites Australis Ash (PAA). *Materials Today: Proceedings,*

Khatib, J., ElKhatib, L., Assaad, J., & El Kordi, A. (2023b). Properties of mortar containing *Phragmites australis* Ash. *Journal of Engineering, Design and Technology*. https://doi.org/10.1108/JEDT-12-2022-0610
Khatib, J., Ramadan, R., Ghanem, H., & Elkordi, A. (2024). Effect of adding *Phragmites-Australis* fiber on the mechanical properties and volume stability of mortar. *Fibers, 12*(2), 14.
Krishna, A., Kaliyaperumal, S. R. M., & Kathirvel, P. (2022). Compressive strength and impact resistance of hybrid fiber reinforced concrete exposed to elevated temperatures. *Structural Concrete, 23*(3), 1611–1624.
Lee, Y., Chun, Y., Kodur, V., & Kim, H. S. (2025). Effect of supplementary cementitious materials on post-fire performance of concrete columns. *International Journal of Concrete Structures and Materials, 19*(1), 49.
Liang, K., Chen, L., & Su, R. K. L. (2025). Bond behavior of basalt fiber-reinforced polymer bars (BFRP) embedded in ultra-high-performance concrete after elevated temperature exposure. *Construction and Building Materials, 481*, Article 141531. https://doi.org/10.1016/j.conbuildmat.2025.141531
Mathew, L., & Paul, M. M. (2017). Mechanical properties of pineapple fibre reinforced concrete subjected to high temperature. *GRD J.—Glob.res. dev.j.eng, 2*, 200–205.
Mihoub, I., Khelifa, M., & Mezhoud, S. (2020). Impact of elevated temperature on the properties of concretes reinforced with Alfa fiber. *Civil and Environmental Engineering Reports, 30*(3), 161–185.
Mohammed, A. D. A. A., Ronghui, W., & Huseien, G. F. (2024). Mechanical properties of natural jute fiber-reinforced geopolymer concrete: Effects of various lengths and volume fractions. *Journal of Composites Science, 8*(11), 450.
Netinger Grubeša, I., Marković, B., Gojević, A., & Brdarić, J. (2018). Effect of hemp fibers on fire resistance of concrete. *Construction and Building Materials, 184*, 473–484. https://doi.org/10.1016/j.conbuildmat.2018.07.014
Noumowe, A. (2005). Mechanical properties and microstructure of high strength concrete containing polypropylene fibres exposed to temperatures up to 200 °C. *Cement and Concrete Research, 35*(11), 2192–2198. https://doi.org/10.1016/j.cemconres.2005.03.007
Othuman Mydin, M. A., Zamzani, N. M., & Ghani, A. N. A. (2019). Experimental data on compressive and flexural strengths of coir fibre reinforced foamed concrete at elevated temperatures. *Data in Brief, 25*, Article 104320. https://doi.org/10.1016/j.dib.2019.104320
Ozawa, M., Kim, G., Choe, G., Yoon, M., Sato, R., & Rokugo, K. (2016). Thermal properties of jute fiber concrete at high temperature. *Journal of Structural Fire Engineering, 7*(3), 182–192. https://doi.org/10.1108/JSFE-09-2016-017
Ramadan, R., Khatib, J., Ghorbel, E., & Elkordi, A. (2023). Effect of adding Phragmites-Australis plant on the chemical shrinkage and mechanical properties of mortar. Paper presented at the *International Conference on Bio-Based Building Materials,* pp. 573–584.
Ridha, M. M. S. (2024). Combined effect of natural fibre and steel fibre on the thermal-mechanical properties of UHPC subjected to high temperature. *Cement and Concrete Research, 180*, Article 107510. https://doi.org/10.1016/j.cemconres.2024.107510
Shon, C., Mukashev, T., Lee, D., Zhang, D., & Kim, J. R. (2019). Can common reed fiber become an effective construction material? Physical, mechanical, and thermal properties of mortar mixture containing common reed fiber. *Sustainability, 11*(3), 903.
Standard, A. (2018). ASTM C33/C33M–18 standard specification for concrete aggregates. *West Conshohocken, PA,*
Talaei, M., & Mostofinejad, D. (2021). Mechanical properties of fiber-reinforced concrete containing waste porcelain aggregates under elevated temperatures. *Construction and Building Materials, 289*, Article 122854. https://doi.org/10.1016/j.conbuildmat.2021.122854
Thomason, J. L., & Rudeiros-Fernández, J. L. (2021). Thermal degradation behaviour of natural fibres at thermoplastic composite processing temperatures. *Polymer Degradation and Stability, 188*, Article 109594. https://doi.org/10.1016/j.polymdegradstab.2021.109594
Ye, H., Zhang, Y., Yu, Z., & Mu, J. (2018). Effects of cellulose, hemicellulose, and lignin on the morphology and mechanical properties of metakaolin-based geopolymer. *Construction and Building Materials, 173*, 10–16. https://doi.org/10.1016/j.conbuildmat.2018.04.028
Zalhaf, N. M. (2025). Application of artificial neural network for prediction of concrete–high-performance concrete interfacial bond strength after exposure to elevated temperature. *International Journal of Concrete Structures and Materials, 19*(1), 31.
Zalhaf, N. M., Fayed, S., & Zakaria, M. H. (2024). Interfacial shear behavior of composite concrete substrate to high-performance concrete overly after exposure to elevated temperature. *International Journal of Concrete Structures and Materials, 18*(1), 19.
Zhang, D., Tan, K. H., Dasari, A., & Weng, Y. (2020). Effect of natural fibers on thermal spalling resistance of ultra-high performance concrete. *Cement and Concrete Composites, 109*, Article 103512. https://doi.org/10.1016/j.cemconcomp.2020.103512
Zhao, H., Zhou, T., Tang, J., Li, Z., Yao, C., & Gao, X. (2025). Temperature-adaptive mechanism of bamboo fibers for regulating elevated temperature performance of UHPC. *Construction and Building Materials, 471*, Article 140674. https://doi.org/10.1016/j.conbuildmat.2025.140674

Publisher's Note

Baydaa Hamdi Salih Baydaa Hamdi Salih holds an MSc in Construction Materials and is a Lecturer in the Department of Civil Engineering at the University of Anbar. Her research interests include sustainable construction materials, cementitious composites, and the development of environmentally friendly building technologies.

Sadoon Abdallah Dr. Sadoon Abdallah holds a PhD in Civil and Environmental Engineering and serves as a Lecturer in the Department of Civil Engineering at the University of Anbar. His research focuses on innovative construction materials, durability of concrete, and the behavior of fiber-reinforced composites under extreme conditions.

Mohammed T. Nawar Mohammed T. Nawar is a PhD student and a Teaching Assistant in the Department of Civil Engineering at the University of Anbar. His academic interests include structural engineering, advanced analysis of reinforced concrete systems, and sustainable construction practices.

Ali J. Ali Ali J. Ali is a PhD student and Teaching Assistant in the Department of Civil Engineering at Brunel University London. His research covers water resources system, structural performance of sustainable composites, and novel engineering applications for bio-based construction materials.

Mizi Fan Professor Mizi Fan is a Professor of Civil and Environmental Engineering at Brunel University London. His research spans bio-based construction materials, sustainable infrastructure systems, and advanced material characterization. He has published extensively in leading international journals and oversees multiple research projects in sustainable engineering.

Ameer A. Hilal Professor Ameer A. Hilal holds a PhD in Civil Engineering and currently serves as the Dean of the College of Engineering at the University of Anbar. His areas of expertise include structural engineering, high-performance concrete, and advanced materials for infrastructure development. He has led several national research initiatives focused on improving construction practices in the region.